Hanbury-Brown–Twiss analysis in a solvable model

G. F. Bertsch,[1,2,*] P. Danielewicz,[3,†] and M. Herrmann[1,‡]
[1] *Institute for Nuclear Theory, HN-12, University of Washington, Seattle, Washington 98195*
[2] *Physics Department, FM-15, University of Washington, Seattle, Washington 98195*
[3] *Department of Physics and Astronomy and National Superconducting Cyclotron Laboratory, Michigan State University, East Lansing, Michigan 48824*
(Received 7 September 1993)

The analysis of meson correlations by Hanbury-Brown–Twiss interferometry is tested with a simple model of meson production by resonance decay. We derive conditions which should be satisfied in order to relate the measured momentum correlation to the classical source size. The Bose correlation effects are apparent in both the ratio of meson pairs to singles and in the ratio of like to unlike pairs. With our parameter values, we find that the single particle distribution is too distorted by the correlation to allow a straightforward analysis using pair correlation normalized by the singles rates. An analysis comparing symmetrized to unsymmetrized pairs is more robust, but nonclassical off-shell effects are important at realistic temperatures.

PACS number(s): 25.75.+r, 21.65.+f, 13.85.Ni

I. INTRODUCTION

An important observable for studying high energy collisions is the momentum correlation between emitted mesons. In the statistical limit the correlation function depends on the Bose symmetry of the particles as in the Hanbury-Brown–Twiss (HBT) analysis of photon correlations from stars (for a review see [1]). Under the statistical assumptions, the meson correlation directly measures the size of the meson interaction zone, and thus indirectly reflects the hadronic dynamics prior to the meson freeze-out. In particular, the correlation between pions and between kaons has been analyzed to give quantitative data on the mean square source dimensions [2–6].

However, the analysis is dependent on the statistical assumptions, raising the question of their validity under realistic conditions of meson production. In this work we develop a simple model of meson production to test the HBT analysis. Within this model we can also examine the concept of a classical source. Before defining the model, we shall briefly review the HBT analysis to establish the notation. The basic observables are the one- and two-particle differential cross sections, $d\sigma^{(1)}/d^3q$ and $d\sigma^{(2)}/d^3q_1 d^3q_2$, within some class of events. Writing the cross section for these events as σ_0, we define the doubles-to-singles correlation function as [7]

$$C^{\mathrm{d/s}}(\boldsymbol{q}_{\mathrm{av}}, \boldsymbol{q}_{\mathrm{rel}}) = \frac{\sigma_0 \dfrac{d\sigma^{(2)}}{d^3q_1 d^3q_2}}{\dfrac{d\sigma^{(1)}}{d^3q_1}\dfrac{d\sigma^{(1)}}{d^3q_2}}. \tag{1}$$

The three-vectors $\boldsymbol{q}_1$ and $\boldsymbol{q}_2$ denote the three-momenta of the two mesons. To facilitate later on the interpretation of the correlation function, we chose the arguments to be the average and relative momentum, $\boldsymbol{q}_{\mathrm{av}} \equiv (\boldsymbol{q}_1 + \boldsymbol{q}_2)/2$ and $\boldsymbol{q}_{\mathrm{rel}} \equiv \boldsymbol{q}_1 - \boldsymbol{q}_2$, respectively.

In the theoretical model, it will be more convenient to express the correlation function using decay rates rather than cross sections. The rates are related to cross sections by a flux factor. In terms of the total decay rate W and the differential decay rates $W^{(2)}(\boldsymbol{q}_1, \boldsymbol{q}_2) = dW/d^3q_1 d^3q_2$ and $W^{(1)}(\boldsymbol{q}) = dW/d^3q$, we evaluate the doubles-to-singles correlation function as

$$C^{\mathrm{d/s}}(\boldsymbol{q}_{\mathrm{av}}, \boldsymbol{q}_{\mathrm{rel}}) = \frac{W\, W^{(2)}(\boldsymbol{q}_1, \boldsymbol{q}_2)}{W^{(1)}(\boldsymbol{q}_1)\, W^{(1)}(\boldsymbol{q}_2)}. \tag{2}$$

To allow an HBT analysis of $C^{\mathrm{d/s}}$, we have to make statistical assumptions (explained in the next section) that reduce the information contained in the two-particle quantities to that contained in the density matrix for a single-particle source. The latter is conveniently expressed in the Wigner representation as the (one-particle) phase space distribution $g^{(1)}(t, \boldsymbol{x}, \omega, \boldsymbol{q})$, where ω is the energy of the meson. The connection to the correlation function is given by Pratt's formula [8], which we will derive in the next section. The formula reads

$$C^{\mathrm{Pratt}}(\boldsymbol{q}_{\mathrm{av}}, \boldsymbol{q}_{\mathrm{rel}}) = 1 + \frac{\int d^4x_1 d^4x_2\, g^{(1)}(x_1, q_{\mathrm{av}}) g^{(1)}(x_2, q_{\mathrm{av}}) \cos q_{\mathrm{rel}}(x_1 - x_2)}{\int d^4x_1 g^{(1)}(x_1, \widetilde{q}_1) \int d^4x_2 g^{(1)}(x_2, \widetilde{q}_2)}. \tag{3}$$

We use a notation here with four-vectors $x = (t, \boldsymbol{x})$ and $q = (\omega, \boldsymbol{q})$. To separate on-shell from off-shell four-momenta we use the notation $\widetilde{q} \equiv (\omega(\boldsymbol{q}), \boldsymbol{q})$ in the on-shell case, where $\omega(\boldsymbol{q}) \equiv \sqrt{\boldsymbol{q}^2 + m_\pi^2}$ is the energy of a

*Internet address: bertsch@phys.washington.edu
†Internet address: danielewicz@nscl.nscl.msu.edu
‡Internet address: herrmann@ben.npl.washington.edu

meson with momentum q and mass m_π. We have also defined the relative and the average four-momenta of the two mesons, $q_{\rm av} \equiv (\tilde{q}_1 + \tilde{q}_2)/2$ and $q_{\rm rel} \equiv \tilde{q}_1 - \tilde{q}_2$.

To compare with theoretical expectations, it is common to model the evolution of the interacting hadronic system using classical transport equations [9–11]. With these simulations one can predict a classical source distribution function, $g^{(1)\rm cl}(t, \boldsymbol{x}, \sqrt{m^2 + \boldsymbol{q}^2}, \boldsymbol{q})$. Note that the energy is not an independent variable in the classical source. Thus in principle there is not enough information to use $g^{(1)\rm cl}$ in Eq. (1), since the required $q_{\rm av}$ in that equation need not have the energy on mass shell. However, in favorable cases the extrapolation off mass shell will not cause difficulties.

We shall also find it useful to analyze the correlation data by dividing the two-particle distribution function by the unsymmetrized two-particle distribution. This is defined

$$C^{\rm l/u}(\boldsymbol{q}_{\rm av}, \boldsymbol{q}_{\rm rel}) = \frac{W^{(2)}(\boldsymbol{q}_1, \boldsymbol{q}_2)}{W_u^{(2)}(\boldsymbol{q}_1, \boldsymbol{q}_2)}, \tag{4}$$

where $W_u^{(2)}$ is the two-particle decay rate in the absence of Bose correlations. These correlations are not present for pairs of unlike mesons, so one could imagine measuring $C^{\rm l/u}$ by, e.g., comparing the correlation between pairs of π^+ mesons to the correlation between π^+ and π^-. We therefore shall call this the like-to-unlike correlation. However, although the Bose interference is absent from the unlike decay distribution, the interaction between unlike mesons induces stronger correlations than for charged mesons of like sign. Another approach to measure $W_u^{(2)}$ is to try to extract it from the correlated data by expressing the rate as a sum of two terms, one the uncorrelated product of two single-particle decays, and the other the correlation. This has been done in some experimental data analyses [12,5]. We will see in this work that it is easier to satisfy the statistical assumptions for the like-to-unlike ratio than for the ratio of doubles to singles.

II. DERIVATION OF THE PRATT FORMULA

The basic formula for the correlation function in terms of the Wigner distribution of the source, Eq. (3), was derived by Pratt assuming an ensemble of classical currents. We will only use quantum mechanical amplitudes, as for example calculated from Feynman diagrams, as it is useful to see what assumptions are necessary to derive the formula from such quantum mechanical expressions.

Our starting point is the symmetrized amplitude

$$T_\alpha^S(q_1, q_2) = T_\alpha^{(2)}(q_1, q_2) + T_\alpha^{(2)}(q_2, q_1) \tag{5}$$

that describes the production of two identical mesons with momentum q_1 and q_2 in some reaction. Thus the events that contribute to the cross section σ_0 are those that produce just two mesons. The label α represents all final state variables that are not observed, such as the number of particles and their momenta. We separate these variables into three sets $\alpha \equiv (\alpha_1|\alpha_2|\alpha_3)$ as follows. In the unsymmetrized amplitude $T^{(2)}_{(\alpha_1|\alpha_2|\alpha_3)}(q_1, q_2)$ the label α_1 denotes the variables that directly influence the production of the meson with momentum q_1, the label α_2 the ones that influence the meson with momentum q_2, whereas α_3 denotes all other variables in the final state.

Up to a possible overall sign, the unsymmetrized amplitude satisfies

$$T^{(2)}_{(\alpha_1|\alpha_2|\alpha_3)}(q_1, q_2) = T^{(2)}_{(\alpha_2|\alpha_1|\alpha_3)}(q_2, q_1). \tag{6}$$

The differential decay rate of the initial state into two mesons is given by

$$W_P^{(2)}(\boldsymbol{q}_1, \boldsymbol{q}_2) \equiv \frac{1}{2}\sum_\alpha \left|T_\alpha^S(\tilde{q}_1, \tilde{q}_2)\right|^2 (2\pi)^4 \delta^4(P_\alpha + \tilde{q}_1 + \tilde{q}_2 - P). \tag{7}$$

Here P denotes the energy-momentum vector of the initial state. P_α is the energy-momentum carried away by all unobserved degrees of freedom. The sum over α represents summation over discrete degrees of freedom and integration over three-momenta, $\int d^3p/(2\pi)^3$. The single-particle decay rate $W^{(1)}$ and W are given by integrals of $W^{(2)}$ over one and over both momenta, respectively.

To obtain expressions for the correlation functions given in Eq. (2) and Eq. (4) we first define the two-particle Wigner function

$$g_P^{(2)}(x_1, q_1; x_2, q_2) = \frac{1}{W_{Pu}}\sum_\alpha \int \frac{d^4p_1 d^4p_2}{(2\pi)^8} e^{-i(p_1x_1 + p_2x_2)} T_\alpha^{(2)}(q_1 + p_1/2, q_2 + p_2/2)\, T_\alpha^{(2)*}(q_1 - p_1/2, q_2 - p_2/2)$$
$$\times (2\pi)^4 \delta^4(P_\alpha + q_1 + q_2 - P). \tag{8}$$

The notation W_{Pu} for the normalization will be explained below. The inverse Wigner transform reads

$$\frac{1}{W_{Pu}}\sum_\alpha T_\alpha^{(2)}(q_1, q_2)\, T_\alpha^{(2)*}(q_3, q_4)\,(2\pi)^4\delta^4\left(P_\alpha + \sum_{i=1}^4 q_i - P\right)$$
$$= \int d^4x_1 d^4x_2 e^{i[(q_1 - q_3)x_1 + (q_2 - q_4)x_2]} g_P^{(2)}\left(x_1, \frac{q_1 + q_3}{2}; x_2, \frac{q_2 + q_4}{2}\right). \tag{9}$$

Inserting (9) into (7) yields

$$\frac{W_P^{(2)}(\boldsymbol{q}_1,\boldsymbol{q}_2)}{W_{Pu}} = \int d^4x_1 d^4x_2 \left[g_P^{(2)}(x_1,\tilde{q}_1;x_2,\tilde{q}_2) + g_P^{(2)}(x_1,q_{\rm av};x_2,q_{\rm av})\cos\left[q_{\rm rel}(x_1-x_2)\right]\right]. \tag{10}$$

We can now express the like-to-unlike correlation function $C^{\rm l/u}$, Eq. (4), in terms of two-particle Wigner functions if we identify the unlike particle production rate with the unsymmetrized two-particle decay rate $W_{Pu}^{(2)}$

$$\begin{aligned} W_{Pu}^{(2)}(\boldsymbol{q}_1,\boldsymbol{q}_2) &= \sum_\alpha \left| T_\alpha^{(2)}(\tilde{q}_1,\tilde{q}_2)\right|^2 (2\pi)^4\delta^4(P_\alpha+\tilde{q}_1+\tilde{q}_2-P) \\ &= \int d^4x_1 d^4x_2\, g_P^{(2)}(x_1,\tilde{q}_1;x_2,\tilde{q}_2)\,. \end{aligned}$$

If we now demand that $g_P^{(2)}$ be normalized for on-shell emission

$$\int d^4x_1 \int d^4x_2 \int \frac{d^3q_1}{(2\pi)^3}\int \frac{d^3q_2}{(2\pi)^3} g_P^{(2)}(x_1,\tilde{q}_1;x_2,\tilde{q}_2) \equiv 1, \tag{11}$$

we see that the normalization factor W_{Pu} introduced in Eq. (8) is just the unsymmetrized total decay rate. We thus find for this correlation function

$$C^{\rm l/u}(\boldsymbol{q}_{\rm av},\boldsymbol{q}_{\rm rel}) = 1 + \frac{\int d^4x_1 d^4x_2 g_P^{(2)}(x_1,q_{\rm av};x_2,q_{\rm av})\cos[q_{\rm rel}(x_1-x_2)]}{\int d^4x_1 d^4x_2 g_P^{(2)}(x_1,\tilde{q}_1;x_2,\tilde{q}_2)}. \tag{12}$$

To get an expression for the correlation function in terms of one-particle quantities [cf. Eq. (3)] the two-particle Wigner function must be factorized into one-particle functions. This demands a number of assumptions. In particular, we require that:

(A1) the unsymmetrized T-matrix factorizes

$$T^{(2)}_{(\alpha_1|\alpha_2|\alpha_3)}(q_1,q_2) = T^{(1)}_{\alpha_1}(q_1)\,T^{(1)}_{\alpha_2}(q_2)\,T^{\rm bath}_{\alpha_3}. \tag{13}$$

This condition can be fulfilled if the production process is dominated by tree graphs. However, this is not enough to factorize Eq. (8), because the δ function still couples the α_1 and α_2 subsystems. So we also assume that:

(A2) the summation over the α_3 degrees of freedom serves as a heat bath that effectively decouples the other two subsystems. Under these two conditions the two-particle Wigner function no longer depends explicitly on the energy and momentum of the initial state but depends on the statistical distribution of energy provided by the integration over α_3. In effect, a microcanonical ensemble is replaced by a canonical ensemble characterized by a temperature in the center-of-mass frame

$$\sum_{\alpha_3}(2\pi)^4\delta^4(P_\alpha+\tilde{q}_1+\tilde{q}_2-P) \sim \exp[(E-P_1^0-P_2^0-\omega_1-\omega_2)/T].$$

We defined P_i^0 to be the energy for the degrees of freedom α_i and $\omega_i \equiv \omega(\boldsymbol{q}_i) \equiv \sqrt{\boldsymbol{q}_i^2+m_\pi^2}$ is the energy of a meson with momentum $\boldsymbol{q}_i$. We label the corresponding Wigner functions g_T, i.e.,

$$g_T^{(1)}(x_1,q_1) = \frac{1}{W_{Tu}}\sum_{\alpha_1}\int \frac{d^4p_1}{(2\pi)^4} e^{-ip_1x_1-(P_1^0+\omega_1)/T} T^{(1)}_{\alpha_1}(q_1+p_1/2)T^{(1)*}_{\alpha_1}(q_1-p_1/2). \tag{14}$$

Then under (A1) and (A2) the two-particle Wigner function factorizes as

$$g_T^{(2)}(x_1,q_1;x_2,q_1) = g_T^{(1)}(x_1,q_1)\,g_T^{(1)}(x_2,q_2)\,. \tag{15}$$

The requirements (A1) and (A2) correspond to the usually cited assumption that the meson field is *chaotic*, i.e., the mesons are created independently. Under these conditions we can now identify the like-to-unlike correlation function, Eq. (4), with Pratt's expression, Eq. (3). However, the two conditions above do not suffice to rewrite the doubles-to-singles correlation function, Eq. (2), in the same way. In addition we have to require that:

(A3) the one-particle decay rate can be calculated neglecting the symmetrization of the amplitude. As this assumption is independent of (A1) and (A2) we can state it in terms of the microcanonically calculated function as defined below Eq. (7),

$$W_P^{(1)}(\boldsymbol{q}_1) \approx W_{Pu}^{(1)}(\boldsymbol{q}_1) = \int \frac{d^3q_2}{(2\pi)^3}\sum_\alpha \left|T_\alpha^{(2)}(\tilde{q}_1,\tilde{q}_2)\right|^2 (2\pi)^4\,\delta^{(4)}(P_\alpha+\tilde{q}_1+\tilde{q}_2-P)\,. \tag{16}$$

A further consequence of (A3) is that the total decay rate W_P can be determined neglecting symmetrization as well, i.e, $W_P \approx W_{Pu}$. It is usually assumed that this condition is fulfilled if typical momenta of the participating particles are large compared to the inverse size of the system, i.e., that the emission processes are sufficiently localized in the emission volume. This condition, however, can be misleading. We will come back to this point in Sec. V.

Given assumption (A3) in addition to (A1) and (A2) the doubles-to-singles correlation function, Eq. (2), can be written using one-particle Wigner functions as in Pratt's expression, Eq. (3).

III. A SOLVABLE MODEL

In this section we will describe a simple model that we use to test how well the assumptions (A1)–(A3) can be fulfilled in a quantum mechanical calculation of meson production by resonance decay. The model is based on a picture of a small source that emits heavy particles. These undergo a cascade of decays to reach the final state. This picture is a plausible one for the decay of the concentrated high energy zone produced by nucleon-antinucleon annihilation or by e^+-e^- annihilation at high energy. The mesonic source would have a spatial extension depending on the initial size of the state and the distance the resonances propagate. In heavy ion collisions, an additional mechanism extending the source is the rescattering of mesons in the later stages of the evolution. In our model, we will permit only the resonance propagation to contribute to the classical source size. The model is thus quite unrealistic for the heavy ion studies, but the criteria we develop have a more general validity.

We will further simplify the resonance cascade process to the Feynman graphs shown in Fig. 1. Here an excitation having definite energy and momentum decays into two resonances and N additional particles. Each resonance propagates and emits a meson into the final state. Only the two mesons are observed; the other particles will be integrated out in calculating the differential decay rates. Note that this graph satisfies the condition (A1) with the three sets of quantum numbers given by the momenta k_1, k_2, and the set p_i.

For computational convenience we assume that all unobserved particles have the same mass m_f, and ignore

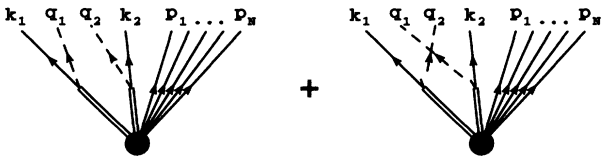

FIG. 1. Graphical representation of the symmetrized amplitude for the production of two mesons in our model.

effects of symmetry among the unobserved particles. We further assume that we can treat the heavy particles nonrelativistically. Their on-shell energy is then given by $\epsilon_f(\boldsymbol{k}) \equiv \boldsymbol{k}^2/2m_f$.

The intermediate resonances are assumed to be represented by simple resonance energy denominators of the form

$$G_r(E,\boldsymbol{P}) \equiv \frac{1}{E-\epsilon_r(\boldsymbol{P})-m_{\rm diff}+i\Gamma_r/2}\,, \tag{17}$$

where $\epsilon_r(\boldsymbol{P}) \equiv \boldsymbol{P}^2/2m_r$, and $m_{\rm diff} \equiv m_r - m_f$ is the difference between resonance mass and the mass of the unobserved particle in the final state. The quantity Γ_r is the width of the resonance. In principle, the coupling constants should be such that the decay rates are consistent with the assumed widths, but since the absolute decay rates play no role we shall ignore this requirement and choose the coupling constant being one.

The couplings at the vertices will be taken as pointlike, since we are ignoring finite sizes of the initial source and of the particles. The meson-production vertices contribute factors of $1/\sqrt{2\omega(\boldsymbol{q})}$ in the perturbation theory. For the numerical calculations, we choose parameters to correspond to the π meson, emitted from the Δ resonance of the nucleon. Accordingly, $m_\pi = 139$ MeV, $m_f = 939$ MeV, $m_r = 1232$ MeV, and $\Gamma_r \equiv \Gamma_\Delta = 115$ MeV. However, note that our assumption of constant form factors corresponds to an s-wave rather than the physical p-wave character of the Δ resonance.

Finally, we will consider only one spatial dimension in the remainder of this work. We will switch to a notation with the space or momentum variables denoted with a Roman letter and the time or energy variable explicitly written out rather than subsumed in a relativistic notation.

The differential decay rate associated with Fig. 1 is given by the following expression:

$$W_P^{(2)}(q_1,q_2)$$

$$= \frac{1}{2}\frac{1}{2\omega(q_1)\,2\omega(q_2)}\int \frac{dk_1}{2\pi}\frac{dk_2}{2\pi}\prod_{j=1}^{N}\frac{dp_j}{2\pi}(2\pi)^2\,\delta\left(E-E_1-E_2-\sum_{i=1}^{N}\epsilon_f(p_i)\right)\delta\left(P-P_1-P_2-\sum_{i=1}^{N}p_i\right)$$

$$\times\left|G_r(E_1,P_1)G_r(E_2,P_2)+G_r[E_1+\omega(q_2)-\omega(q_1),P_1+q_2-q_1]G_r[E_2+\omega(q_1)-\omega(q_2),P_2+q_1-q_2]\right|^2\,. \tag{18}$$

For notational convenience we have defined quantities

$$E_i \equiv \epsilon_f(k_i)+\omega(q_i) \tag{19}$$

and

$$P_i \equiv q_i + k_i \tag{20}$$

corresponding to the resonance energies and momenta, respectively. In the next section we will examine how this expression approaches W_T as the number of particles N gets large.

IV. THERMAL LIMIT

Our first application of the model will be to see how the thermal limit is approached as the number of spectator particles increases. We first define the spectator phase space volume by integrating the delta functions in Eq. (18) over the spectator momenta p_j,

$$\Omega^{(N)}(E,P) \equiv \int \frac{dp_1 \cdots dp_N}{(2\pi)^N} (2\pi)^2 \delta\left(E - \sum_{i=1}^{N} \epsilon_f(p_i)\right) \delta\left(P - \sum_{i=1}^{N} p_i\right). \tag{21}$$

This may be evaluated in closed form to obtain[1]

$$\Omega^{(N)}(E,P) = K\left(E - \frac{P^2}{2Nm_f}\right)^{\frac{N-3}{2}}. \tag{22}$$

Here K is a constant that we calculated but, as the expression is complicated and will drop out later on, we do not show it here. Inserting this in Eq. (18), the two-particle probability distribution can be evaluated as a double integral. Before presenting the numerical results it is useful to see how the thermal limit arises. When N is large we may write the needed phase space function as

$$\Omega^{(N)}(E - E_1 - E_2, P - P_1 - P_2) \approx \Omega^{(N)}(E,P) \exp\left[-N\left(E_1 + E_2 - (P_1 + P_2)\frac{P}{m_f N}\right) \Big/ 2E^*\right],$$

where $E^* = E - P^2/2m_f N$ is the center-of-mass energy. From here on we shall consider momenta in the frame where $P \equiv 0$. The effective temperature associated with the phase space is then $T = 2E/N$, as expected from the equipartition theorem for N degrees of freedom.

We now compare the doubles-to-singles correlation function evaluated explicitly from the finite-N two-particle probability function Eq. (18), and the corresponding thermal limit,

$$W_T^{(2)}(q_1,q_2)$$

$$= \frac{\Omega^{(N)}(E,P=0)}{2} \frac{1}{2\omega(q_1)\,2\omega(q_2)} \int \frac{dk_1}{2\pi}\frac{dk_2}{2\pi} \exp\left[-(E_1+E_2)/T\right]$$
$$\times \left|G_r(E_1,P_1)G_r(E_2,P_2) + G_r[E_1 + \omega(q_2) - \omega(q_1), P_1 + q_2 - q_1]G_r[E_2 + \omega(q_1) - \omega(q_2), P_2 + q_1 - q_2]\right|^2. \tag{23}$$

Figure 2 shows typical results for $C^{\mathrm{d/s}}$ calculated with Eqs. (18) and (23). The total energy was chosen to be $E = 1.5\,m_\pi N$ corresponding to a temperature of $T = 3\,m_\pi$, which is the temperature used in Eq. (23). The correlation function is shown as a function of the momentum difference $q_{\mathrm{rel}} = q_1 - q_2$ for fixed average momentum $q_{\mathrm{av}} = 0$. It may be seen that the finite-N correlation function approaches the result of the thermal limit. So we conclude that as few as 50 participating particles justify the assumption that the correlation function can be calculated using a canonical ensemble instead of a microcanonical one. We expect that in three dimensions the same heat bath would require of the order of 20 particles.

V. THE SINGLES DISTORTION

It is immediately apparent from Fig. 2 that the correlation function looks quite different from the expected form, which should start at 2 at zero q_{rel} and fall monotonically to 1 at large q_{rel}. We can trace this behavior back to a violation of condition (A3). In Fig. 3 we show $W_T^{(1)}$ (full line) calculated by integrating over the symmetrized $W_T^{(2)}$ as compared to an integral over the unsymmetrized $W_{Tu}^{(2)}$ (dashed line) [cf. Eqs. (7) and (16)]. The two curves clearly deviate strongly for small values of q. It is obvious that also the total particle production probability cannot be calculated neglecting symmetriza-

[1]The N-fold integration can only be done analytically for nonrelativistic particles.

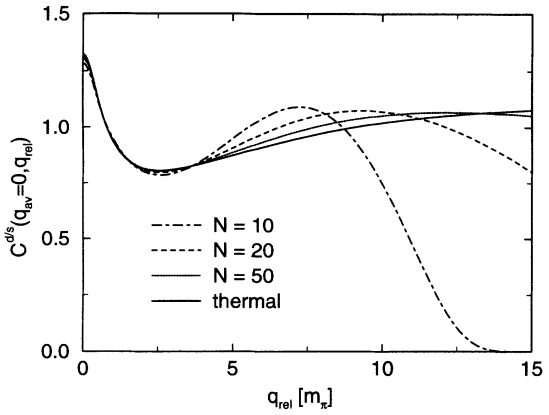

FIG. 2. Correlation function $C^{d/s}$ for different numbers of particles and in the thermal limit. The energy is $E = 1.5Nm_\pi$ which corresponds in the thermal limit to a temperature of $T = 3\,m_\pi$. The average momentum of the meson pair is zero for all cases.

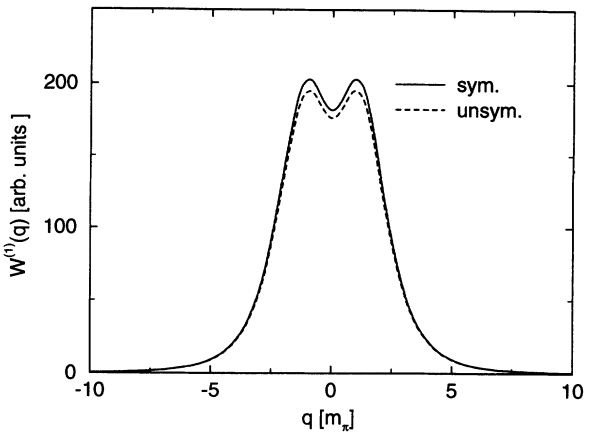

FIG. 4. Same as Fig. 3, but for a small resonance width $\Gamma_r = \Gamma_\Delta/10$.

tion. These facts account for the *wrong* asymptotic values of the correlation function. To make things worse the correlation function has a pronounced dip for intermediate values of $q_{\rm rel}$. That means that even the introduction of an overall normalization factor and a coherence parameter λ does not help to extract the desired information about the source from $C^{d/s}$.

The validity of (A3) can be determined empirically [12]. The single-particle distribution is evaluated by integrating over one of the two momenta in the two-particle distribution function Eq. (10) or (23). The contribution of the interference term is of the order of the width of the correlation function Δq_c divided by a typical momentum difference $\langle (q_1 - q_2)^2 \rangle^{1/2}$. This should be small for (A3) to hold. From Fig. 2 we have $\Delta q_c \approx 3/4m_\pi$ and Fig. 3 gives $\langle (q_1 - q_2)^2 \rangle^{1/2} \approx 3m_\pi$, yielding

$$\frac{\Delta q_c}{\langle (q_1 - q_2)^2 \rangle^{1/2}} \approx 25\%. \tag{24}$$

This is intolerably large to ignore in the HBT analysis.

One might anticipate that in three dimensions the relevant expression would be the cube of Eq. (24), which would make (A3) a rather good assumption. However, analysis of experimental data shows distortions of the order of 10% [5]. Also in a Fritiof Monte Carlo simulation of NA35 data [13] an influence of the symmetrization of the singles spectrum of 10–20 % was found. Coming back to our model, we find that by decreasing the width of the resonance down to $\Gamma_r = \Gamma_\Delta/10$ we actually decrease Δq_c so much that (A3) becomes valid. In Fig. 4 we show the single-particle decay rate again for the symmetrized (full line) and unsymmetrized (dashed line) two-particle amplitude. Compared to Fig. 3 the deviation of the two curves is very small. Indeed the calculation of the doubles-to-singles correlation function yields a satisfactory result, shown in Fig. 5 (full line). The small deviation from two at low $q_{\rm rel}$ and one for high $q_{\rm rel}$ is due to the residual small difference between the single-particle decay rate in the symmetrized and the unsymmetrized case, respectively, as well as numerical inaccuracy in evaluating the two-particle decay rate for such a small resonance width. In Fig. 5 we show also

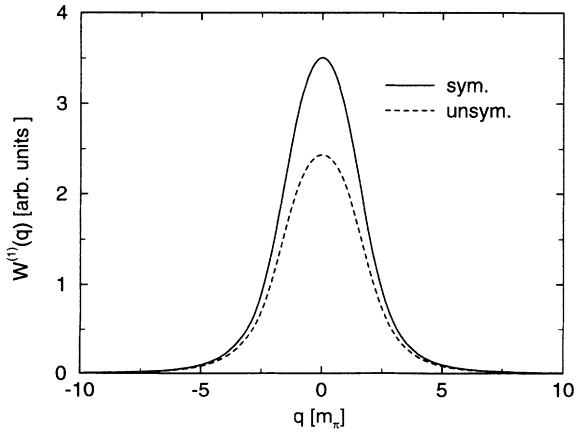

FIG. 3. Single-particle decay rate $W^{(1)}(q)$ calculated with the symmetrized (full line) and unsymmetrized (dashed line) two-particle amplitude, for $T = 3m_\pi$ and $\Gamma_r = \Gamma_\Delta$.

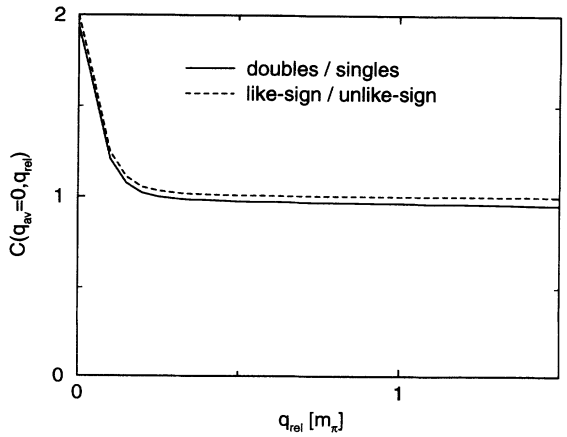

FIG. 5. The correlation functions $C^{d/s}$ (full line) and $C^{l/u}$ (dashed line) for a resonance width $\Gamma_r = \Gamma_\Delta/10$ and $T = 3m_\pi$.

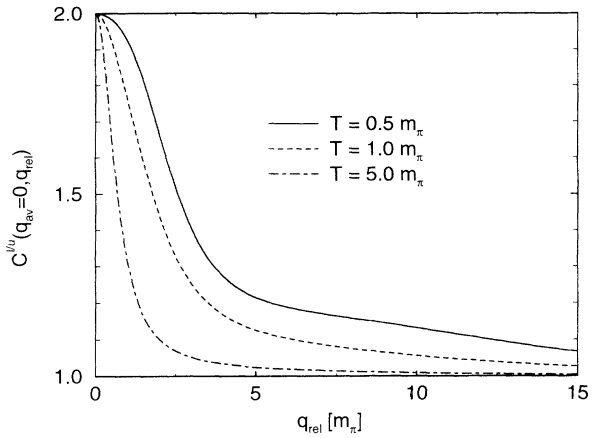

FIG. 6. The correlation function $C^{l/u}$ for different temperatures $T = 0.5m_\pi$ (full line), $1.0m_\pi$ (dashed line), and $5.0m_\pi$ (dot-dashed line). The width of the resonance is $\Gamma_r = \Gamma_\Delta$.

the like-to-unlike correlation function $C^{l/u}$ for the same parameters (dashed line). As expected for the case of a small singles distortion we find a good agreement of the two correlation functions.

VI. SOURCE SIZES

In the remainder of this work we shall concentrate on the measure $C^{l/u}$ to avoid the problem of the distortion in the singles spectrum. In Fig. 6 we show the thermal model $C^{l/u}$ for parameters corresponding to the physical Δ resonance and for several values of the temperature. The correlation function is seen to be well behaved, and one can try to extract source size parameters from the width of the peak. Notice that the peak becomes narrower as the temperature increases. This seems to indicate that the emitting system is larger for higher temperatures. We will discuss this point in detail in Sec. VI B. We now address the question of whether a classical source size can be extracted from the peak width.

A. Classical limit

We first derive the classical limit of the one-particle Wigner function for our model. The Wigner transform of the quantum amplitude has the form

$$g_T^{(1)}(t,x,\omega_{\rm av},q_{\rm av}) = \int \frac{dk}{2\pi} e^{-[\omega_{\rm av}+\epsilon_f(k)]/T} \int \frac{d\omega_{\rm rel}}{2\pi}\frac{dq_{\rm rel}}{2\pi} e^{-i(\omega_{\rm rel}t-q_{\rm rel}x)} \left[2\omega(q_1)\,2\omega(q_2)\right]^{-1/2} \times G_r\left[\epsilon_f(k)+\omega_{\rm av}+\omega_{\rm rel}/2, k+q_1\right] G_r^*\left[\epsilon_f(k)+\omega_{\rm av}-\omega_{\rm rel}/2, k+q_2\right]. \quad (25)$$

The integration over $\omega_{\rm rel}$ can be performed by an ordinary contour integration. The contribution from the two poles is

$$g_T^{(1)}(t,x,\omega_{\rm av},q_{\rm av}) = \Theta(t) \int \frac{dk}{2\pi} e^{-[\omega_{\rm av}+\epsilon_f(k)]/T} \int \frac{dq_{\rm rel}}{2\pi} e^{iq_{\rm rel}x} \left[2\omega(q_1)\,2\omega(q_2)\right]^{-1/2} \times \frac{2ie^{-\Gamma t}}{E_+ + E_-}\left[\exp(-2iE_+t) - \exp(2iE_-t)\right], \quad (26)$$

where

$$E_\pm = \epsilon_r(k+q_{\rm av} \pm q_{\rm rel}/2) + m_{\rm diff} - \epsilon_f(k) - \omega_{\rm av}. \quad (27)$$

Up to this point the calculation is still exact, i.e., Eq. (26) still contains the full quantum mechanical information. We now derive a classical source function by approximations on the above expression. We first expand $E_\pm$ to first order in the momentum difference $q_{\rm rel}$

$$E_\pm \approx \Delta E \pm \left.\frac{d\epsilon_r(p)}{dp}\right|_{p=q_{\rm av}+k} q_{\rm rel}/2, \quad (28)$$

where

$$\Delta E = \epsilon_r(k+q_{\rm av}) + m_{\rm diff} - \epsilon_f(k) - \omega_{\rm av}. \quad (29)$$

The derivative $d\epsilon_r(p)/dp$ is the classical velocity $v_r(p)$ of the resonance. Thus we may write

$$g_T^{(1){\rm cl}}(t,x,\omega_{\rm av},q_{\rm av}) = \frac{\Theta(t)}{\omega(q_{\rm av})} e^{-\Gamma_r t} \int \frac{dk}{2\pi} e^{-[\omega_{\rm av}+\epsilon_f(k)]/T} \int \frac{dq_{\rm rel}}{2\pi} e^{i[q_{\rm rel}x - qtv_r(k+q_{\rm av})]} \frac{\sin(2\Delta Et)}{\Delta E}. \quad (30)$$

The integral over $q_{\rm av}$ gives a δ function and the last factor approaches the δ function $2\pi\delta(\Delta E)$. Therefore the classical approximation amounts to demanding that the resonance propagates on-shell. Evaluating the δ functions and dropping the subscript "av" we obtain

$$g_T^{(1){\rm cl}}(t,x,\omega,q) = \frac{\Theta(t)}{\omega(q)} e^{-\Gamma_r t} \sum_{i=1,2} \delta\left[x - v_r\left(k_f^i+q\right)t\right] e^{-\left(k_f^i+q\right)^2/2m_rT} \frac{1}{\left|v_r\left(k_f^i+q\right) - v_f\left(k_f^i\right)\right|}. \quad (31)$$

In this equation, k_f^1 and k_f^2 are the two roots of the condition $\Delta E = 0$, which resulted from the evaluation of the k integral over the delta function $\delta(\Delta E)$. These roots are solutions of a quadratic equation and are given by

$$k_f^{1,2} \equiv \frac{m_f}{m_{\rm diff}} q \pm \sqrt{\frac{m_f m_r}{m_{\rm diff}^2} q^2 + 2 m_f m_r \left(1 - \frac{\omega}{m_{\rm diff}}\right)}. \tag{32}$$

The k integral gives the density-of-states factor at the end of Eq. (31). Note that the various terms in this Wigner function (except the density-of-states factors) have obvious classical interpretations. The initial Θ function specifies that the source starts at $t = 0$, and its exponential decay is given by the second factor. The resonance propagates classically with connection between its position, velocity, and the time given by the argument of the delta function. The probability to make the resonance is given by the Boltzmann factor following. With this one-particle Wigner function in the classical approximation we can evaluate the classical correlation function $C^{\rm cl}$ by inserting $g_T^{(1)\rm cl}$, Eq. (31), into Pratt's expression, Eq. (3).

Note that our classical $g_T^{\rm cl}$ depends on the variables q and ω independently. Figure 7 shows the correlation as a function of $q_{\rm rel}$ with average momentum fixed at $q_{\rm av} = 0$ and temperature $T = m_\pi$, indicated by the solid curve. The correlation function behaves as expected for small momentum differences. For large momenta, however, $C^{\rm cl}$ develops a singularity. This can be traced back to the occurrence of $\omega_{\rm av}$ in the argument of the Wigner functions in the numerator of Eq. (3). Under sufficiently extreme conditions, this energy goes off-shell so far that the classical condition $\Delta E = 0$ no longer has a solution. If $\omega_{\rm av}$ is replaced by an on-shell energy, namely by $\omega(q_{\rm av})$, the problem does not arise. The correlation function calculated with this on-shell prescription is shown as the dashed curve. This function is very similar to the original one for small $q_{\rm rel}$. In contrast to the singular behavior of the original correlation function the dotted curve behaves smoothly also for high $q_{\rm rel}$. Since this problem arises at high momentum, and the source size question depends on the low momentum behavior only, we can ignore the differences for the remainder of this work.

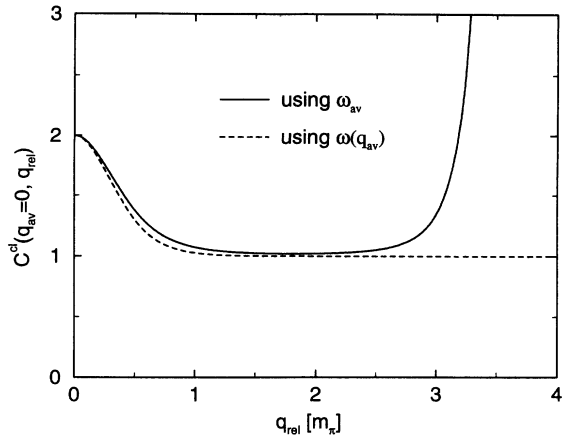

FIG. 7. Classical correlation function with different treatments of the energy variable, for $T = 1\,m_\pi$ and $\Gamma_r = \Gamma_\Delta$.

B. Contributions to the source size

A convenient way to characterize the information contained in the correlation function is to take the second derivative with respect to the momentum difference at $q_{\rm rel} = 0$. This gives an effective mean square source size defined as

$$\langle x^2 \rangle^{\rm eff} \equiv -\frac{1}{2} \left. \frac{d^2 C}{dq_{\rm rel}^2} \right|_{q_{\rm rel}=0}. \tag{33}$$

We determine this from the single-particle Wigner source function taking the derivative of Eq. (3). This yields

$$\langle x^2 \rangle^{\rm eff} = \left[\frac{1}{G} \int dt\, dx \left[x - v_\pi(q_{\rm av})\, t\right]^2 g - \left(\frac{1}{G} \int dt\, dx \left[x - v_\pi(q_{\rm av})\, t\right] g \right)^2 - \left(\frac{1}{2G} \frac{dG}{dq_{\rm av}} \right)^2 + \frac{1}{4G} \frac{d^2 G}{dq_{\rm av}^2} - \frac{1}{4G} \left. \frac{d^2 \omega(q)}{dq^2} \right|_{q=q_{\rm av}} \frac{\partial}{\partial \omega} \int dt\, dx\, g(t, x, \omega, q_{\rm av})|_{\omega=\omega(q_{\rm av})} \right]. \tag{34}$$

In writing this we used the abbreviations $g = g^{(1)}[t, x, \omega(q_{\rm av}), q_{\rm av}]$ and $G = \int dt\, dx\, g^{(1)}[t, x, \omega(q_{\rm av}), q_{\rm av}]$. The quantity v_π is the velocity of the pion $v_\pi(q) \equiv d\omega(q)/dq$. We will refer to the five contributions of the right-hand side of Eq. (34) by $\langle x^2 \rangle^I, \ldots, \langle x^2 \rangle^V$ respectively. $\langle x^2 \rangle^I$ and $\langle x^2 \rangle^{II}$ correspond to the space-time distribution of the emission points of the mesons. This is the information we would like to extract. The other terms give corrections which are due to the energy and momentum dependence of the source.

To simplify the discussion we concentrate on the behavior at $q_{\rm av} = 0$. Then $\langle x^2 \rangle^{II}$ and $\langle x^2 \rangle^{III}$ in Eq. (34) vanish by symmetry. The first term is easily evaluated with the classical source $g_T^{(1)\rm cl}$ [Eq. (31)]. The result is

$$\langle x^2 \rangle_{\rm cl}^I = \frac{1}{G} \int dt\, dx \left[x - v_\pi(q_{\rm av})\, t\right]^2 g_T^{(1)\rm cl} = 2 \left(\frac{k_f^0 / m_r}{\Gamma_r} \right)^2, \tag{35}$$

where k_f^0 is the classical momentum of the resonance required to emit a meson at $q = 0$. It is given by [compare Eq. (32)]

$$k_f^0 \equiv \sqrt{2m_f m_r \left(1 - \frac{m_\pi}{m_{\rm diff}}\right)}. \tag{36}$$

The result Eq. (35) is of course exactly what one would expect for a source moving with velocity k_f^0/m_r and decaying at a rate Γ_r.

Note also that the source size is independent of the temperature. This is counterintuitive at the first glance. However, in the classical approximation the momentum of the resonance is kinematically fixed by the momentum of the emitted pion. Therefore the distance the resonance travels before it emits the pion is determined only by the kinematics and lifetime.

C. Comparison of classical and quantum results

We now extract the source size from the quantum mechanical thermal source. The correlation function at $q_{\rm av} = 0$ has the form

$$C^{\rm l/u}(q_{\rm av} = 0, q_{\rm rel}) = 1 + \frac{|\mathcal{I}_T(q_{\rm rel}, -q_{\rm rel})|^2}{\mathcal{I}_T(q_{\rm rel}, q_{\rm rel})\,\mathcal{I}_T(-q_{\rm rel}, -q_{\rm rel})} \tag{37}$$

where

$$\mathcal{I}_T(q_1, q_2) = \int dk\; e^{-[\epsilon_f(k)+\omega(q_1/2)]/T} G_r[\epsilon_f(k) + \omega(q_1/2), k + q_1/2]\; G_r^*[\epsilon_f(k) + \omega(q_2/2), k + q_2/2]. \tag{38}$$

It is straightforward to evaluate $\mathcal{I}$ by contour integration. The result in the $T \to \infty$ limit is particularly simple, yielding for the correlation function

$$C_\infty^{\rm l/u}(q_{\rm av} = 0, q_{\rm rel}) = 1 + \frac{1}{\left(1 + (q_{\rm rel}/q_0)^2\right)^2}, \tag{39}$$

where we have defined

$$q_0 \equiv {\rm Im}\sqrt{\frac{m_r}{m_f} q_{\rm rel}^2 + 8\frac{m_{\rm diff} m_r}{m_f}\,[m_{\rm diff} - \omega(q_{\rm rel}/2) - i\Gamma_r/2]}. \tag{40}$$

The source size may be evaluated from Eq. (33). In the limit $\Gamma_r \ll m_{\rm diff} - m_\pi$, it reduces exactly to the classical formula, Eq. (35),

$$\langle x^2\rangle_q^{\rm eff} \approx \langle x^2\rangle_{\rm cl}^I. \tag{41}$$

At finite temperature, the expression for $C^{\rm l/u}$ is rather unwieldy and we quote only the source size, obtained either directly from Eq. (33) or with Eq. (34) and the quantum Wigner function Eq. (25). The quantum mean square radius $\langle x^2\rangle_q^{\rm eff}$ is found to be

$$\langle x^2\rangle_q^{\rm eff} = \left\langle\!\!\left\langle \frac{(v_r - v_\pi)^2}{(\Delta E)^2 + (\Gamma_r/2)^2} \right\rangle\!\!\right\rangle - \left| \left\langle\!\!\left\langle \frac{v_r - v_\pi}{\Delta E + i\Gamma_r/2} \right\rangle\!\!\right\rangle \right|^2. \tag{42}$$

Here we used $\Delta E = \epsilon_r(k + q_{\rm av}) + m_{\rm diff} - \epsilon_f(k) - \omega(q_{\rm av})$ and the thermal average $\langle\langle f\rangle\rangle$ weighted by the resonance distribution is defined as

$$\langle\langle\, f\,\rangle\rangle \equiv \frac{\int dk\; e^{-\epsilon_f(k)/T} f \left((\Delta E)^2 + (\Gamma_r/2)^2\right)^{-1}}{\int dk\; e^{-\epsilon_f(k)/T} \left((\Delta E)^2 + (\Gamma_r/2)^2\right)^{-1}}. \tag{43}$$

In Fig. 8 we show the mean square source size for a width of the resonance $\Gamma_r = \Gamma_\Delta$ and $q_{\rm av} = 0$. Note that for vanishing average momentum only the first term on the right-hand side of Eq. (42) contributes. The quantum mean square radius $\langle x^2\rangle_q^{\rm eff}$ is shown as a function of temperature, indicated by the solid line. This is compared to the temperature-independent classical size $\langle x^2\rangle_{\rm cl}^I$ indicated by the dashed line. It might be hoped that the additional terms in Eq. (34) would improve the classical description, but this is not the case. The full classical source size $\langle x^2\rangle_{\rm cl}^{\rm eff}$, shown as the dot-dashed line, in fact deviates in the opposite direction from the quantum result. The disagreement is serious, since we are interested in temperatures of the order of $T = m_\pi$ and lower, for

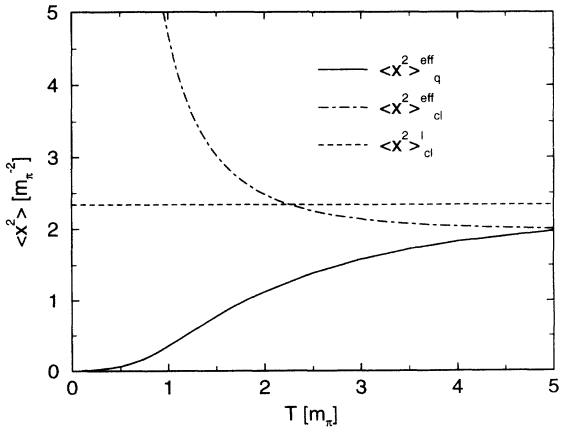

FIG. 8. The mean square source size as a function of the temperature in various treatments. The horizontal dashed line is the classical size $\langle x^2\rangle_{\rm cl}^I$, Eq. (35). The dot-dashed curve includes corrections to the size of the classical source from Eq. (34). The solid line gives the result from the quantum mechanical calculation, Eq. (42). The width is $\Gamma_r = \Gamma_\Delta$.

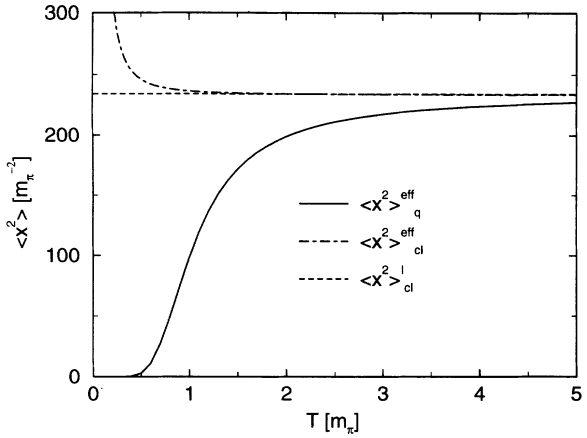

FIG. 9. Same as Fig. 8 but for the reduced width $\Gamma_r = \Gamma_\Delta/10$.

physical sources.

Clearly, the off-shell propagation is important at physically realizable temperatures. Even for widths that might seem small, the exponential factor in Eq. (43) emphasizes states with low energy in Eq. (42). This is illustrated in Fig. 9, showing the source size for a very small width, $\Gamma_r = \Gamma_\Delta/10$. We see that even in this case the classical source is unreliable for temperatures below $2m_\pi$. The problem is severe because in the classical calculation a zero-momentum pion is not produced from a low momentum resonance as is favored in the quantum mechanical calculation. However, if we choose conditions such that the resonance region is not suppressed by the Boltzmann factor, the classical source is accurate down to much lower temperatures.

Even though our model calculation shows that quantum effects are important for the interferometry among mesons produced by resonances, our result Eq. (42) suggests a way to improve classical modeling. When particles propagate far off-shell, their lifetime is controlled by $(\Delta E)^{-1}$, according to the uncertainty principle, rather than by Γ_r^{-1}. Equation (42) could be recovered from a classical simulation if in Eq. (35) the resonance lifetime Γ_r^{-1} is replaced by an effective lifetime $\sim [(\Gamma_r/2)^2 + (\Delta E)^2]^{-1/2}$, with a suitable averaging over an ensemble of resonances with different ΔE's.

VII. SUMMARY

We have studied a resonance decay model to test the statistical assumptions behind the HBT analysis of meson correlations. One set of assumptions gives rise to a reduction of the unsymmetrized two-particle source function to a product of two single-particle thermal sources. We find that it is not too difficult to realize conditions that substantially satisfy this statistical assumption. The usual HBT analysis requires, however, that the single-particle distribution be calculable from an unsymmetrized two-particle source, and this condition is much more difficult to fulfill.

For resonance decays, we can ask whether the correlation reflects the spatial propagation of the resonances before they decay. We find that the apparent source size extracted from the quantum mechanically calculated correlation function deviates strongly from the classical mean square size even for resonance parameters and temperatures that suggest a classical behavior. The off-shell propagation of resonances is important and needs to be taken account of in the classical propagation if extracted source sizes are to make sense.

ACKNOWLEDGMENTS

This work has been supported in part by the Department of Energy under Grant DE-FG06-90ER40561 (G.B., M.H.), by the National Science Foundation under Grants PHY90-17077 and PHY89-04035 (P.D.), and by the Alexander von Humboldt-Stiftung (Feodor-Lynen Program) (M.H.).

[1] D. Boal, C. K. Gelbke, and B. Jennings, Rev. Mod. Phys. **62**, 553 (1990).
[2] T. Åkesson *et al.*, Z. Phys. C **36**, 517 (1987).
[3] D. Ferenc *et al.*, Nucl. Phys. **A544**, 531c (1992); P. Seyboth *et al.*, *ibid.* **A544**, 293c (1992).
[4] J. P. Sullivan, M. Berenguer, B. V. Jacak, S. Pratt, M. Sarabura, J. Simon-Gillo, H. Sorge, and H. van Hecke, Phys. Rev. Lett. **70**, 3000 (1993).
[5] H. Bøggild *et al.*, Phys. Lett. B **302**, 510 (1993).
[6] Y. Akiba *et al.*, Phys. Rev. Lett. **70**, 1057 (1993).
[7] M. Gyulassy, S. K. Kaufmann, and L. W. Wilson, Phys. Rev. C **20**, 2267 (1979).
[8] S. Pratt, Phys. Rev. Lett. **53**, 1219 (1984).
[9] S. Pratt, Phys. Rev. D **33**, 1314 (1986).
[10] G. Bertsch, M. Gong, and M. Tohyama, Phys. Rev. C **37**, 1896 (1988).
[11] M. Gyulassy and S. Padula, Phys. Lett. B **217**, 181 (1989).
[12] W. Zajc *et al.*, Phys. Rev. C **29**, 2173 (1984).
[13] K. Kadija and P. Seyboth, Phys. Lett. B **287**, 363 (1992).